



OPEN ACCESS

EDITED BY

Geraldine Zimmer-Bensch,
RWTH Aachen University, Germany

REVIEWED BY

Júlio Santos Terra Machado,
Federal University of Rio Grande do Sul, Brazil
Randy J. Kulesza,
Lake Erie College of Osteopathic
Medicine, United States
Mona K. Roesler,
Johannes Kepler University of Linz,
Austria

*CORRESPONDENCE

Zhaoming Wei
weizhaoming@snnu.edu.cn
Yingfang Tian
yingfang_tian@snnu.edu.cn

SPECIALTY SECTION

This article was submitted to
Cellular Neuropathology,
a section of the journal
Frontiers in Cellular Neuroscience

RECEIVED 30 September 2022

ACCEPTED 23 November 2022

PUBLISHED 08 December 2022

CITATION

Liu Y, Di Y, Zheng Q, Qian Z, Fan J,
Ren W, Wei Z and Tian Y (2022)
Altered expression of glycan patterns
and glycan-related genes
in the medial prefrontal cortex of the
valproic acid rat model of autism.
Front. Cell. Neurosci. 16:1057857.
doi: 10.3389/fncel.2022.1057857

COPYRIGHT

© 2022 Liu, Di, Zheng, Qian, Fan, Ren,
Wei and Tian. This is an open-access
article distributed under the terms of
the [Creative Commons Attribution
License \(CC BY\)](https://creativecommons.org/licenses/by/4.0/). The use, distribution
or reproduction in other forums is
permitted, provided the original
author(s) and the copyright owner(s)
are credited and that the original
publication in this journal is cited, in
accordance with accepted academic
practice. No use, distribution or
reproduction is permitted which does
not comply with these terms.

Altered expression of glycan patterns and glycan-related genes in the medial prefrontal cortex of the valproic acid rat model of autism

Yingxun Liu^{1,2,3}, Yuanyuan Di², Qi Zheng², Zhaoqiang Qian²,
Juan Fan^{1,2}, Wei Ren⁴, Zhaoming Wei^{1,2*} and Yingfang Tian^{1,2*}

¹Key Laboratory of Ministry of Education for Medicinal Plant Resource and Natural Pharmaceutical Chemistry, National Engineering Laboratory for Resource Developing of Endangered Chinese Crude Drugs in Northwest of China, College of Life Sciences, Shaanxi Normal University, Xi'an, Shaanxi, China, ²College of Life Sciences, Shaanxi Normal University, Xi'an, Shaanxi, China, ³Genetic Engineering Laboratory, College of Biological and Environmental Engineering, Xi'an University, Xi'an, Shaanxi, China, ⁴School of Education, Shaanxi Normal University, Xi'an, Shaanxi, China

Autism spectrum disorders (ASD) represent a group of neurodevelopmental defects characterized by social deficits and repetitive behaviors. Alteration in Glycosylation patterns could influence the nervous system development and contribute to the molecular mechanism of ASD. Interaction of environmental factors with susceptible genes may affect expressions of glycosylation-related genes and thus result in abnormal glycosylation patterns. Here, we used an environmental factor-induced model of autism by a single intraperitoneal injection of 400 mg/kg valproic acid (VPA) to female rats at day 12.5 post-conception. Following confirmation of reduced sociability and increased self-grooming behaviors in VPA-treated offspring, we analyzed the alterations in the expression profile of glycan patterns and glycan-related genes by lectin microarrays and RNA-seq, respectively. Lectin microarrays detected 14 significantly regulated lectins in VPA rats, with an up-regulation of high-mannose with antennary and down-regulation of Sia α 2-3 Gal/GalNAc. Based on the KEGG and CAZy resources, we assembled a comprehensive list of 961 glycan-related genes to focus our analysis on specific genes. Of those, transcription results revealed that there were 107 differentially expressed glycan-related genes (DEGGs) after VPA treatment. Functional analysis of DEGGs encoding anabolic enzymes revealed that the process trimming to form core structure and glycan extension from core structure primarily changed, which is consistent with the changes in glycan patterns. In addition,

the DEGs encoding glycoconjugates were mainly related to extracellular matrix and axon guidance. This study provides insights into the underlying molecular mechanism of aberrant glycosylation after prenatal VPA exposure, which may serve as potential biomarkers for the autism diagnosis.

KEYWORDS

glycan-related genes, glycan patterns, valproic acid, autism, mPFC

Introduction

Autism spectrum disorder (ASD) are characterized by early-onset difficulties, including social deficits, and abnormally restricted and repetitive behaviors (American Psychiatric Association, 2013; Muhle et al., 2018). To date, the exact pathophysiology and molecular mechanism of autism still remain unclear, because of the complex interplay of environmental and genetic factors that determine susceptibility (Kuo and Liu, 2018; Muhle et al., 2018). Gene-environment interactions may influence the expression of genes that are mainly related to neuronal activity and synapse development during the early stage of brain development (Mabunga et al., 2015; Varghese et al., 2017). Thus, pathophysiological processes in ASD seem to converge on specific molecular networks and pathways, with a precise regulation in the formation and function of brain synapses (Quesnel-Vallieres et al., 2019).

Glycosylation is one of the most common and frequent post-translational protein modifications (Maupin et al., 2010). Glycans and their conjugates (glycoproteins, proteoglycans, and glycolipids) are the major constituents of the neural extracellular matrix (ECM) (Dwyer and Esko, 2016; Schjoldager et al., 2020). In this context, glycosylation can influence the nervous system in various ways by affecting the functions of glycoproteins involved in nervous system development and physiology (Mutalik and Gupton, 2021). The production of glycan and glycoconjugate is governed by a series of glycan biosynthesis and catabolic enzymes. In contrast, alterations in the expression of these critical enzymes sensitively reflect the glycosylation patterns, cell morphology, and pathogenesis of neurodevelopmental disorders, including ASD (Blanchard et al., 2012; Irie et al., 2012; Pearson et al., 2013; Freeze et al., 2015; Yang et al., 2018; Demirci et al., 2019; Oinam et al., 2020; Yang et al., 2020). Demirci et al. (2019) provided evidence that the levels of salivary sialic acid (Sia) in children with ASD were statistically lower than those in healthy controls. Furthermore, the expression of the *GNE* gene, which encodes UDP-GlcNAc2-epimerase/ManNAc kinase, a key enzyme in Sia biosynthesis, was reported to be negatively correlated with stereotypical behaviors in children with ASD (Yang et al., 2018, 2020). Heparan sulfate proteoglycan is

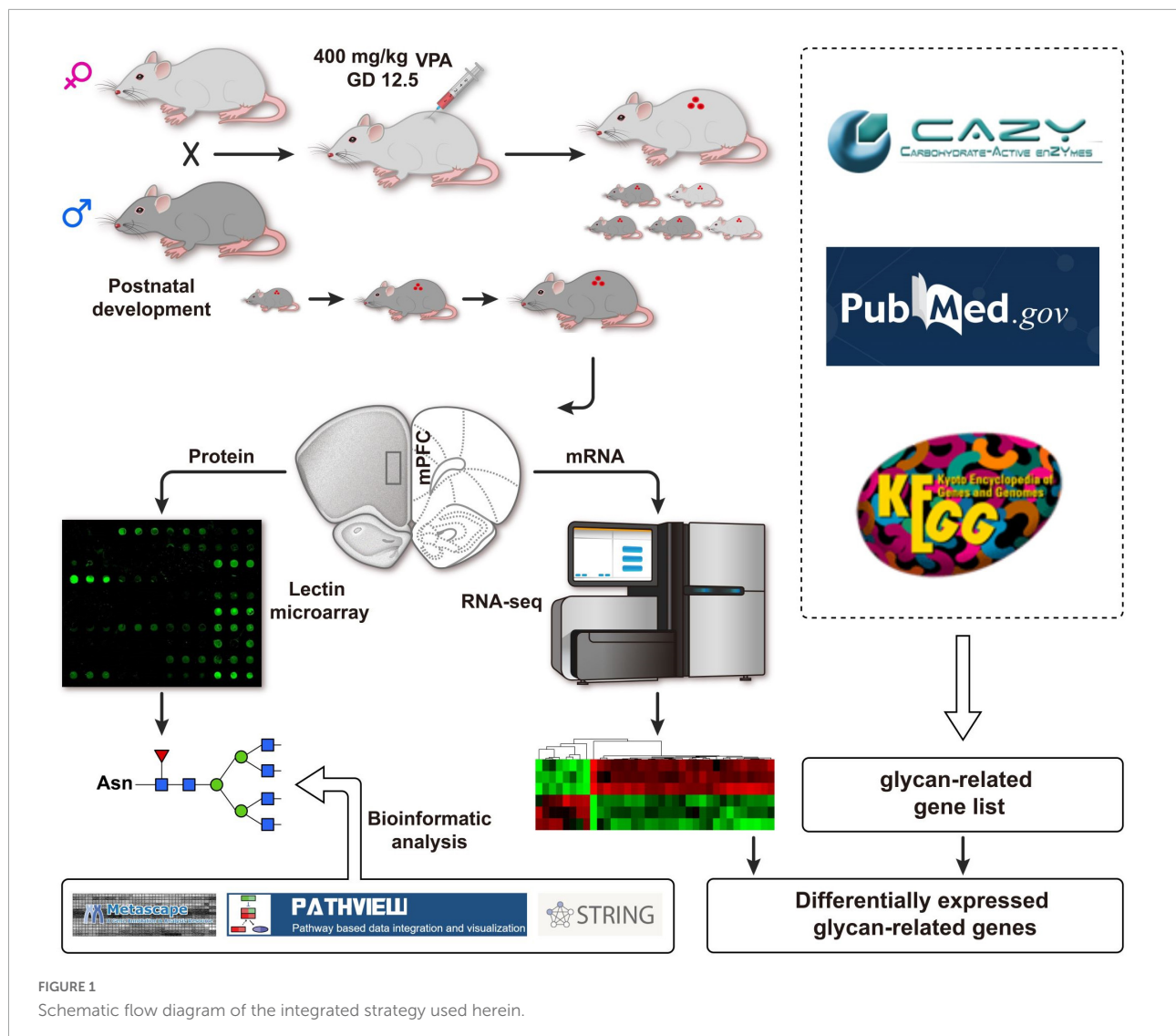
one of the major components of the ECM, which is tightly connected to the intracellular environment, and required for cortical neurogenesis and axon guidance (Dwyer and Esko, 2016). Pagan et al. reported a reduction in the levels of heparan sulfate in young to mature autistic patients' brain lateral ventricles (Pearson et al., 2013). These data agrees with previous findings from the BTBR T+tf/J mouse, a kind of inbred strain mice which displays an ASD-like behavioral phenotype (Blanchard et al., 2012), and with mice with genetic modifications reducing heparan sulfate (Irie et al., 2012). Thus, recent studies indicated that the aberrant protein glycosylation is potentially involved in the molecular mechanism of ASD patients and the genetic animal model of ASD.

Embryonic exposure to valproic acid (VPA) in rodents is the most frequently used environmentally triggered autism model, which appropriately replicates disturbed behaviors, including social deficits and repetitive behaviors seen in ASD (Mabunga et al., 2015). VPA is non-specific histone deacetylase (HDAC) inhibitor and regulates gene transcription through chromatin remodeling (Fukuchi et al., 2009; Lucchina and Depino, 2014; Olde Loohuis et al., 2017; Zhang et al., 2018; Tartaglione et al., 2019). Therefore, we hypothesized that VPA treatment might cause the expression of glycan-related genes, which may contribute to protein glycosylation and affect perineuronal nets. As shown in **Figure 1**, we combined glycomics and transcriptomics analysis to systematically identify the aberrant expression of glycan patterns and glycan-related genes in a VPA-induced rat model of autism, which may provide useful insights into autism pathogenesis, and serve as potential biomarkers for autism diagnosis (Kuo and Liu, 2018).

Materials and methods

Valproic acid-induced rat model of autism

Sprague-Dawley rats were purchased from Xi'an Jiaotong University animal center (Xi'an, China). All rats were housed under a 12-h light/dark cycle at 18–22°C, relative humidity at



50–60%, and allowed free access to food and water. All animal experiments were performed under the National Institutional Animal Care and the guidelines approved by the Animal Care and Use Committee of Shaanxi Normal University (2019-021). All efforts were made to minimize the number of animals used and their suffering, and the spare rats were euthanized by carbon dioxide asphyxiation by using animal euthanasia device with the condition of 70% of the chamber or cage volume/min.

The VPA-induced rat model of autism was carried out as previously reported (Zhou et al., 2016; Zhang et al., 2018). Female rats (250–300 g) were mated overnight, the vaginal secretion was collected the next morning, and the day on which spermatozoa were detected was designated the first day of gestation (GD1). Pregnant female rats ($n = 12$) were randomly grouped into control ($n = 5$) and VPA groups ($n = 7$). The VPA group received a single intraperitoneal injection of 400 mg/kg VPA (250 mg/ml in saline, pH 7.3.

Sigma, Oakville, CA) on GD 12.5, while the control group was injected with saline. The offspring were weaned on a postnatal day (PND) 23 and separated by sex. Only male offspring were used in the current study (Zhang et al., 2018). To minimize the litter-specific effects, only 1–2 animals per litter were used in the behavioral experiment, and one animal per litter was used in other analyses. All experiments were performed in a blinded manner in order to prevent subjective bias.

Behavioral testing

To confirm the autistic-like behaviors in rats prenatally exposed to VPA, the social behaviors and repetitive behaviors tests were performed from PND 30–35 on VPA ($n = 11$), and saline ($n = 8$) treated dams. The social behaviors test was

performed using the three-chamber test as previously described (Wu et al., 2020; Di et al., 2021). Rats were individually acclimated for 5 min in the three-chamber apparatus 1 day before the test. At the beginning of the sociability test, the test rat was introduced into the center of the middle chamber for 5 min habituation. Then, an age- and sex-matched unfamiliar stimulus Sprague-Dawley rat (stranger) was placed in one of the side cages. The sociability test was performed for 10 min by placing the test rat into the middle chamber. Sociability was evaluated by the sociability index (SI), which was defined as the ratio of the duration of the test rat on the novel rat side to that on the empty side.

A self-grooming test was performed to estimate repetitive behaviors. Each rat was placed in a clean empty plastic cage (46 × 32 × 20 cm) and habituated for 10 min. The bedding was not used to prevent digging behavior. Then, the subject rat was recorded for cumulative time spent on self-grooming during the 10-min testing period. Grooming was defined as rubbing the face, body, or head with the two forelimbs.

Medial prefrontal cortex collection

After the behavioral tests, animals were euthanized with 10 g/L with pentobarbital sodium (40 mg/kg) intraperitoneally. The mPFC region (AP = 3.7~2.2 mm; ML = 0~1.2 mm; DV = -2~-5.0 mm) was dissected from both hemispheres according to the previous protocols with minor modifications (Völgyi et al., 2017; Sang et al., 2018). These tissues were rapidly frozen in liquid nitrogen and used for total protein and RNA extraction, respectively.

Lectin microarrays and data analysis

Three male rats from VPA-exposed and control groups, were selected for lectin microarray. The mPFC tissue was harvested, and total proteins were extracted by lysing cells with PBST buffer (10 mM PBS (pH7.4), 140 mM NaCl, 2.7 mM KCl, 1% Triton X-100). The supernatant was collected after centrifugation at 14,000 × *g* for 20 min at 4°C. Following the protein concentration assay, equal amounts of proteins from different experiments were labeled with Cy5.5 fluorescence dye (GE Healthcare; Perry Hall, MD, USA) according to the manufacturer's instructions. Briefly, Cy5.5 fluorescence dye was dissolved in DMSO for 0.5 h at room temperature, and it was incubated with proteins in 0.1 M Na₂CO₃ solution (pH 9.3) for 2.5 h at room temperature. The reaction was terminated by the addition of 4 M hydroxylamines for 10 min at 4°C. The Cy5.5 labeled proteins were purified by Sephadex G-25 columns, and applied to the lectin microarray.

The manufacture of lectin microarray and data acquisition was performed as described previously (Yu et al., 2012; Qin et al., 2017). Briefly, 4 μg of Cy5.5-labeled proteins were mixed with 0.5 mL of hybridization buffer and were incubated with the lectin microarray at 20°C overnight. Microarrays were washed with probing pad three times and centrifuged to dry. Finally, the microarrays were scanned using a GenePix 4000B confocal scanner. The GenePix Pro 3.0 software program extracted numerical data from the scanned images. The average background was subtracted, and values less than the average background ± 2 standard deviations (SD) were removed from each data point. The median of the effective data points for each lectin was globally normalized to the sum of the medians for all of the practical data points in one block. Each sample was consistently observed from three repeated slides. The normalized data of the VPA group and the control group were then compared to determine any relative change in protein glycosylation levels.

Transcriptomic analysis of glycan-related genes expression

The expression profiles of glycan-related genes were analyzed by using RNA-seq with RNA isolated from the mPFC tissue of three VPA-exposed rats and control rats, respectively. The preparation of sequencing libraries, Illumina HiSeq2000 sequencing, and RNA-seq data processing were performed as described previously and following the manufacturer's instructions (Zhang et al., 2018). Sample description has been deposited in the BioSample Submission Portal as Bioproject PRJNA397961, and complete data sets have been submitted to the Sequence Read Archive database¹ under accession numbers SRR5950172 to SRR5950177. Gene expression in VPA-exposed rats was compared to saline-treated controls, and analysis was done using the DESeqR package. Genes with false discovery rate (FDR) adjusted *p*-value < 0.05 were assigned as differentially expressed genes (DEGs).

Compilation of the glycan-related gene list

To focus our analysis on specific genes, we selectively analyzed the transcriptomics data from a target glycan-related genes list based on several sources, including Kyoto Encyclopedia of Genes and Genomes (KEGG²), Carbohydrate Active Enzymes (CAZy³), and National Center

¹ <https://www.ncbi.nlm.nih.gov/sra>

² <https://www.genome.jp/kegg/>

³ <http://www.cazy.org/>

TABLE 1 Organization of the rat glycan-related gene list.

Group	Family or subgroup	No.	Source
Enzymes			
Glycosyltransferases	CAZy families: GT1-4, GT6-8, GT10-14, GT16-18, GT21-25, GT27, GT29, GT31-GT32, GT35, GT39, GT41, GT43, GT50, GT54, GT57-59, GT61, GT64-66, GT68, GT90, GT98, GT110, GT NC	259	CAZy
Glycoside hydrolases	CAZy families: GH1-2, GH13, GH18, GH20, GH22, GH27, GH29-31, GH33, GH35, GH37-38, GH47, GH56, GH59, GH63, GH65, GH79, GH84, GH99, GH116	94	CAZy
Carbohydrate-binding modules	CAZy families: CBM20-21, CBM48, CBM57	7	CAZy
Glycan biosynthesis and metabolism	N-Glycan biosynthesis	12	KEGG
	Various types of N-glycan biosynthesis	2	KEGG
	Mannose type O-glycan biosynthesis	5	KEGG
	Glycosaminoglycan biosynthesis	78	KEGG
	Glycosaminoglycan degradation	6	KEGG
	Glycosylphosphatidylinositol (GPI)-anchor biosynthesis	20	KEGG
	Glycosphingolipid biosynthesis-ganglio series	1	KEGG
	Other glycan degradation	1	KEGG
Proteins			
Lectins	C-Type, I-type, L-type, M-type, P-type, S-type, F-box lectins, Calnexin/calreticulin, Chitinase-like lectins, Intelectins	128	KEGG: Lectins
Glycosylphosphatidylinositol (GPI)-anchored proteins	Enzymes	18	KEGG
	Receptors	16	KEGG
	Antigens	67	KEGG
	Others	15	KEGG
Proteoglycans	Cell surface proteoglycans	12	KEGG
	ECM proteoglycans	36	KEGG
Glycosaminoglycan binding proteins	Heparan sulfate/Heparin	166	KEGG
	Hyaluronan	18	KEGG

for Biotechnology Information (NCBI⁴) (see **Table 1** for gene list categories, member totals, and sources). Unique NCBI gene identifiers (GeneIDs) for each member of the gene list were used to check for isoforms of a single gene to prevent duplications of gene entries in the list. Genes that encode anabolic enzymes with multiple functions were grouped by their catalytic activity to avoid redundant entries. Genes with adjusted *p*-value < 0.05 were assigned as differentially expressed glycan-related genes (DEGGs).

Verification by quantitative real-time PCR

Quantitative real-time PCR analysis was used to validate the glycan-related gene identified by RNA-seq. The sequence of gene-specific primers employed in the analysis is presented in **Table 2**. qRT-PCR was performed in CFX96TM Real-Time System (Bio-Rad, Hercules, CA, USA) as previously described

(Zhang et al., 2018). Each PCR process was followed by a general dissociation curve protocol to check product specificity. All samples were run in biological triplicate, and the average values were calculated. The mRNA expression of the target gene was calculated by the $\Delta\Delta$ CT method, and β -actin was employed as the reference gene, which is the main component of cytoskeletal protein with stable expression through various conditions.

Analysis of biological processes of genes encoding anabolic enzymes

Functional analysis was performed by using Metascape⁵ tool to gain insights into functional groupings within the set of identified differentially expressed glycan-related genes. For the presentation of the expression profile data, fold change (FC) of the DEGGs encoding anabolic enzymes were uploaded to the Pathview web⁶ to gain color pathway visualization

⁴ www.ncbi.nlm.nih.gov

⁵ <http://metascape.org/gp/>

⁶ <https://pathview.uncc.edu/>

TABLE 2 Primers and amplicon characteristics for the evaluated genes.

Gene symbol	Accession number	Primer sequences	Amplicon size/bp
<i>Large1</i>	NM_001108439.1	TCCTTGGCTGACCAGGACAT AGAGAGCCAGACTGATGGGT	200
<i>Man2a2</i>	XM_008759529.3	TCTGTCTTAGCCTGCGCATC AGAGGGCGGAGGCGG	116
<i>St6gal2</i>	XR_005488860.1	CTCCTGCAGCACAGCACTT TTGTTCCAGACTCTGGCGGAC	231
<i>Galnt9</i>	XM_039089515.1	CAACCAGCTGAATGAACGCT TCGTGGGTGGCTGTGATTTT	122
<i>Hs3st5</i>	NM_001106392.1	GCCGAGCATCCAAACTACT ACTCTGTCTCACCCTGTGTC	127
<i>Actin</i>	NM_031144.3	TGACAGGATGCAGAAGGAGA TAGAGCCACCAATCCACACA	104

(Luo et al., 2017). The symbol nomenclature for glycans was used to visualize the glycan structures (Neelamegham et al., 2019).

Protein interaction network analysis of genes encoding glycoconjugates

Protein interaction network analysis was performed as previously described (Cao et al., 2021). Briefly, protein interaction networks were extracted from the STRING database⁷ using a confidence cut-off of 0.4 (medium confidence level in STRING) for target genes encoding glycoconjugates. Markov cluster (MCL) was performed on the network in Cytoscape using Clustermaker2. For each functional neighbor gene cluster, we conducted gene ontology (GO) and KEGG pathway enrichment analysis using the Cytoscape plugin BiNGO based on universal GO, and KEGG annotation terms. The significant enriched biological processes (BP), molecular functions (MF), cellular component (CC), and KEGG pathway were highlighted with FDR value.

Statistical analysis

GraphPad Prism 8 software (GraphPad Software, La Jolla, CA, USA) was used to generate descriptive statistics, perform statistical comparisons, and graph all continuous variables of behavioral testing. The normality test was performed by the Shapiro-Wilk test. Data sets that fit a normal distribution ($p > 0.05$) were compared using the standard unpaired *t*-test to determine significant differences between the two groups. When the *p*-value was less than 0.05, it was considered that the difference was statistically significant.

⁷ <https://cn.string-db.org/>

Results

Prenatal exposure to valproic acid results in autistic-like behaviors

Three-chamber test was employed to elucidate the social behavior deficits in the rat offspring prenatally exposed to VPA (Figure 2A). In the sociability stage of the test (Figure 2B), the control rats spent more time in the stranger chamber than those in the empty section [$t(14) = 6.996$, $P < 0.0001$], whereas the rats in the VPA group showed no significant difference in the time duration between the stranger and empty chamber [Stranger 220.5 ± 36.5 , Empty 233.4 ± 23.4 ; $t(20) = 0.9867$, $P = 0.3356$]. Thus, the rats in the VPA group demonstrated a significant decrease in the social index compared with those in the control group [$t(17) = 5.374$, $P < 0.0001$]; (Figure 2C). In self-grooming test (Figure 2D), VPA-treated rats showed a significant increase in total time spent self-grooming compared to the saline-injected controls [VPA 126.8 ± 36.5 , Control 48.9 ± 13.0 ; $t(17) = 6.104$, $P < 0.0001$]. Taken together, rat offspring prenatally exposed to VPA at E12.5 exhibited autistic-like behaviors, including social deficits and repetitive behaviors.

Alteration of glycan patterns in the valproic acid-induced model of autism

To estimate the alteration of the glycosylation state after prenatal VPA exposure, the proteins were extracted from the mPFC of VPA-treated and saline-treated control rats and subjected to lectin microarrays. The layout of the lectin microarray, and the resulting glycopatterns defined by the microarrays for the VPA-treated and control groups are shown in Figures 3A,B. There were 14 lectins that significantly changed ($FC \geq 1.2$ or ≤ -1.2) in VPA-treated rats compared to negative controls (Figure 3C; Table 3). Of those, ConA ($FC = 1.82$) and

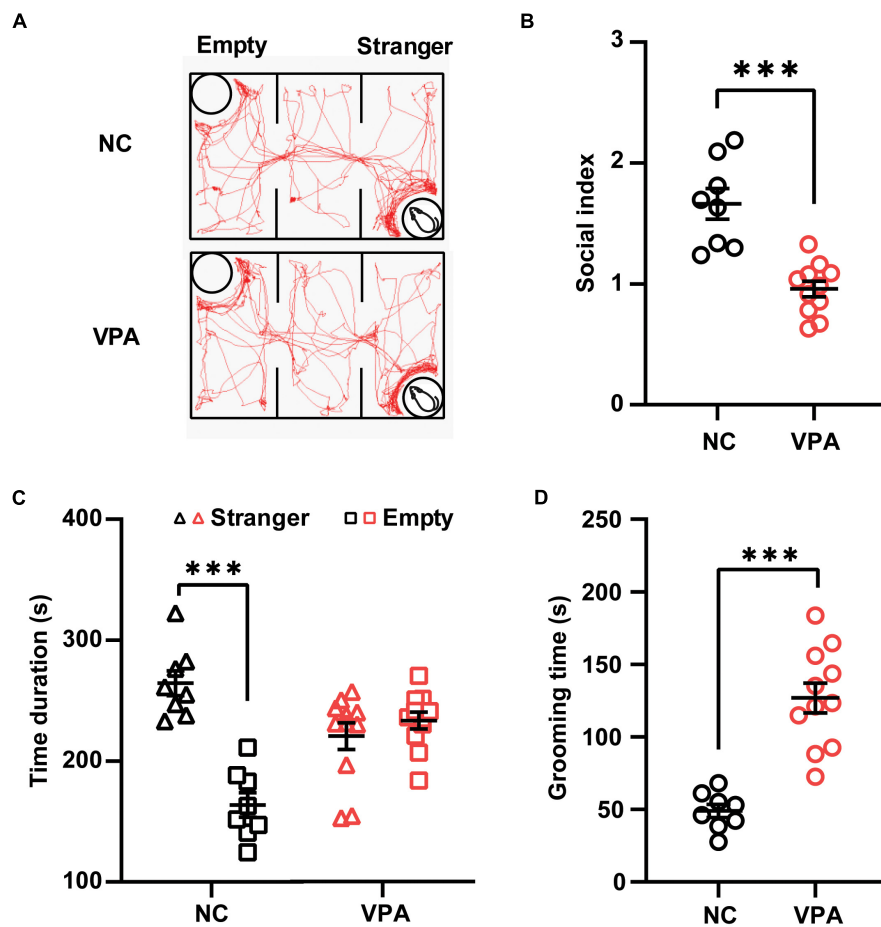


FIGURE 2

Effects of prenatal exposure to valproic acid (VPA) on autistic-like behaviors in male offspring. (A) Track of rat offspring in the social test of the three-chamber test. Quantification of time duration (B) and the social index (C) in the social test showed decreased social behaviors of VPA-exposed offspring. (D) VPA-exposed offspring spent significantly more time on self-grooming during the 10-min test session. *** $p \leq 0.001$.

GNA (FC = -3.34) were the two most significantly up-regulated and down-regulated lectins, respectively. Although both bind to high mannose, the subtle mannose structure is different. ConA mainly binds branched mannose, while GNA specifically recognizes terminal α -1, 3 mannose, suggesting the modest mannose structure changed significantly in VPA-exposed rats. The remaining significantly changed lectins also included 4 GlcNAc-binding lectins (GSL-II, PHA-E, DSA, and WGA), 3 GalNAc-binding lectins (PTL-I, DBA, and VVA), 5 Galactose-binding lectins (ECA, Jacalin, MAL-I, BPL, and RCA120). Based on the specificity of lectin-recognized structures, the results of lectin microarrays revealed that complex-type N-glycan with antennary (recognized by GSL-II and PHA-E) was up-regulated. In contrast, the Sia α 2-3 Gal/GalNAc (recognized by WGA and MAL-I) and terminal GalNAc structure (recognized by BPL and VVA) were down-regulated in VPA rats. In summary, lectin microarray results indicated that the glycan patterns of glycoproteins, especially the subtle high-mannose structure,

were significantly altered in an environmentally triggered autism model.

Assembly of the glycan-related gene list

To examine the global regulation of glycan abundance in rat brain tissue, we first generated a comprehensive list of glycan-related genes, which included genes encoding glycosyltransferases (GTs), glycoside hydrolases (GHs), anabolic enzymes related to glycosylation, and glycan-binding proteins. For assembly of the gene list, numerous web-based resources were chosen, predominantly CAZy database³ and KEGG glycan.⁸ We first added the 259, 94, and 7 rats genes encoding GTs, GHs, and carbohydrate-binding modules, respectively,

⁸ <http://www.genome.jp/kegg/glycan/>

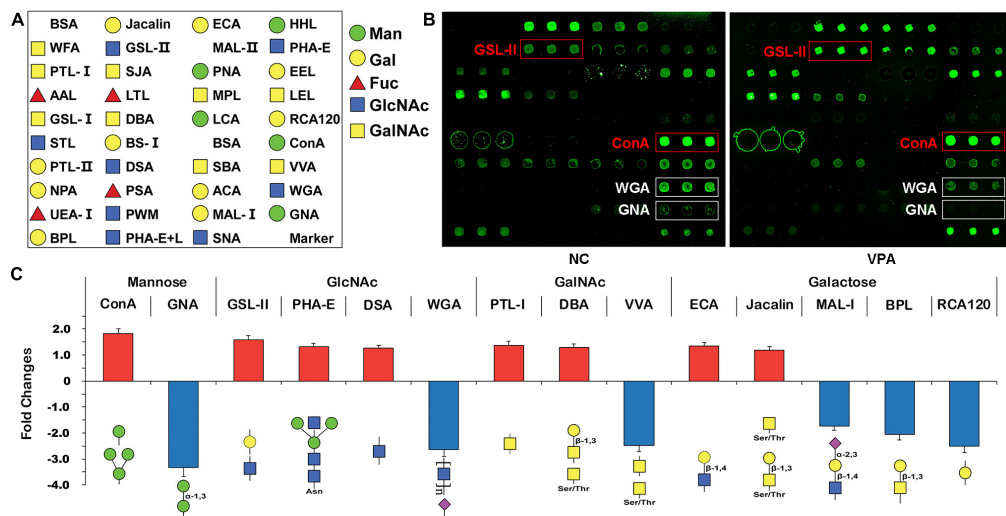


FIGURE 3

Glycan profiling of valproic acid (VPA) rats and negative control using lectin microarrays. (A) The layout of the lectin microarray. Each lectin is printed in triplicate. (B) Scanned images were derived by analysis of VPA rats and negative control. The substantially altered lectins [concanavalin A (ConA), *Griffonia simplicifolia* II (GSL-II), wheat germ agglutinin (WGA), and *Vicia villosa* agglutinin (VVA)] are marked with white boxes. (C) Fold change of normalized fluorescence intensity (NFI) of 14 lectins with significant differences in lectin microarray. NFI is the ratio of the median of the effective data points for each lectin to the sum of the medians for all of the practical data points for each lectin in one block. Lectins with fold change ≥ 1.2 or ≤ -1.2 were assigned as up-regulation or down-regulation.

that are registered in the CAZy database (Nairn et al., 2008). Subsequently, 125 genes encoding anabolic enzymes other than GTs or GHs were added, such as genes involved in N-Glycan and O-glycan biosynthesis, Glycosaminoglycan biosynthesis and degradation, Glycosylphosphatidylinositol (GPI)-anchor biosynthesis and Glycosphingolipid biosynthesis. Finally, 476 genes encoding glycan-binding proteins (lectins), Proteoglycans, GPI-anchored Proteins, or Glycosaminoglycan Binding Proteins were accumulated from the KEGG glycan database. In total, 961 rat genes were collected and categorized into eight groups. The complete list of rat glycan genes, including gene list categories, member totals, and sources, is contained in Table 1.

Identification of differentially expressed glycan-related genes in valproic acid-induced rat model of autism

To explore the causes of the alteration in glycan patterns, we used RNA sequencing to investigate transcriptome in the prefrontal cortex of VPA-exposed rats, and found 3,228 differentially expressed genes in VPA rats compared to controls (adjusted p -value < 0.05) (Figure 4A; Zhang et al., 2018). To focus our analysis on specific genes, we generated a comprehensive rat glycan-related gene list based on the KEGG glycan and CAZy database (Kanehisa et al., 2016). Of these 961 glycan-related genes, the mRNA levels of 107 genes

significantly changed in VPA-treated rats (Supplementary Table 1). As shown in Figure 4A, most DEGs fall under glycosyltransferases (27 genes, 25.2%) and glycosaminoglycan binding proteins (28 genes, 26.1%). More information about these DEGs was further categorized according to their specific functions and listed in Tables 4, 5.

Among these 107 DEGs, 27 genes were ≤ -1.5 fold down-regulated in the VPA-treated group, whereas eight genes were ≥ 1.5 fold up-regulated. The expression of these DEGs with fold change of more than 1.5 fold was visualized as a heat map using MeV cluster software (Figure 4B). Notably, the color-based view demonstrated these DEGs exhibiting the most significant fold change were clustered side-by-side in the dendrogram. To confirm the outcome of the RNA sequencing, we determined expression levels of 5 DEGs (*Large1*, *Man2a2*, *St6gal2*, *Galnt9*, and *Hs3st5*) by qRT-PCR (Figure 4C). These genes were selected mainly because they have been reported as candidate genes related to autism. In VPA rats, the expression of 4 genes (*Large1*, *Man2a2*, *St6gal2*, and *Galnt9*) was significantly decreased, and the presentation of *Hs3st5* was greatly increased, which was consistent with results from RNA-seq.

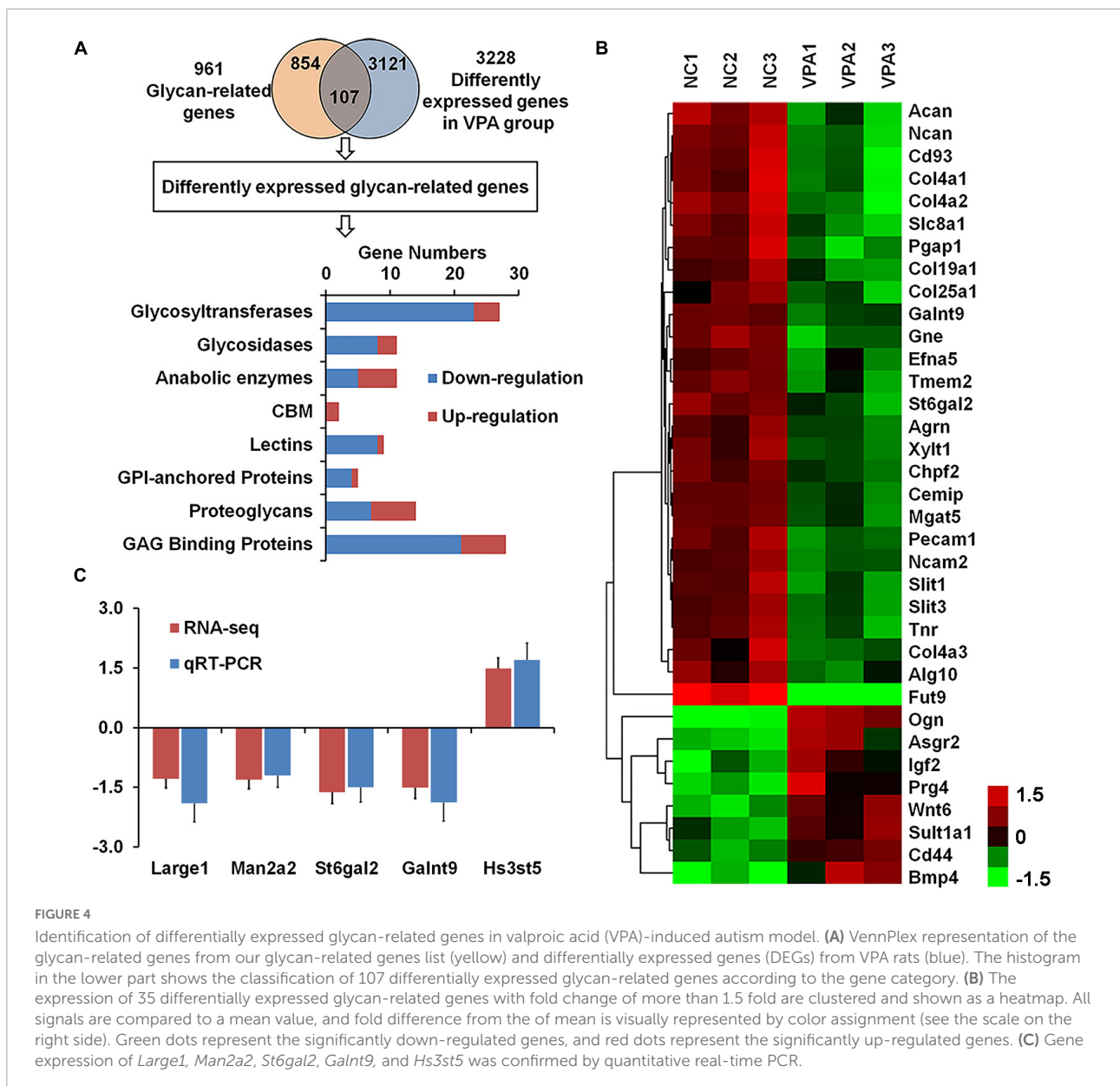
Integration of gene expression of anabolic enzymes and glycan patterns

For clarity, these DEGs were divided into two categories: one is genes encoding enzymes involved in glycosylation, and the other is genes encoding glycoconjugates.

TABLE 3 Changes in glycan structure recognized by 14 different lectins in valproic acid (VPA)-induced autism model.

Mono-saccharide	Lectin	Specificity	Binding structure	NFI		FC
				CON	VPA	
Mannose	ConA	Branched and terminal Man; terminal GlcNAc High-mannose, Man α 1-6 (Man α 1-3)Man		0.109	0.198	1.82
	GNA	High-mannose; Man α 1-3Man		0.020	0.006	-3.34
GlcNAc	GSL-II	GlcNAc and agalactosylated tri/tetra antennary glycans		0.059	0.094	1.59
	PHA-E	Bisecting GlcNAc, biantennary complex-type N-glycan with outer Gal		0.031	0.040	1.32
GalNAc	DSA	β -D-GlcNAc, (GlcNAc β 1-4) _n , Gal β 1-4GlcNAc		0.027	0.034	1.26
	WGA	Multivalent Sia and (GlcNAc) _n		0.083	0.031	-2.63
	PTL-I	GalNAc; GalNAc α -1,3Gal β -1,3/4Glc		0.042	0.058	1.38
	DBA	GalNAc α -Ser/Thr(Tn); GalNAc α 1-3((Fuc α 1-2))Gal		0.006	0.008	1.29
Galactose	VVA	terminal GalNAc; GalNAc α -Ser/Thr(Tn), GalNAc α 1-3Gal		0.071	0.029	-2.47
	ECA	Gal β -1,4GlcNAc (type II); Gal β 1-3GlcNAc (type I)		0.054	0.072	1.34
	Jacalin	Gal β 1-3GalNAc α -Ser/Thr(T); GalNAc α -Ser/Thr(Tn)		0.102	0.122	1.20
	MAL-I	Sia α 2-3Gal β 1-4Glc(NAc), Sia α 2-3Gal		0.024	0.014	-1.72
	BPL	Gal β 1-3GalNAc; Terminal GalNAc		0.049	0.024	-2.06
	RCA120	β -Gal, Gal β -1,4GlcNAc (type II), Gal β 1-3GlcNAc (type I)		0.024	0.009	-2.50

NFI, Normalized fluorescent intensity; FC, Fold change.



Functional enrichment analysis revealed that these 51 DEGs encoding anabolic enzymes primarily affected the N-glycan biosynthesis pathway (KEGG: rno00510). As shown in **Figure 5A**, members of the process of trimming to form the core structure and glycan extension from core structure were significantly downregulated in VPA rats, including *Man1a2*, *Man2a2*, *Mgat3*, *Mgat5*, and *St6gal2*. These results suggest that the synthesis of N-glycans might be inhibited in VPA-treated rats, which may be responsible for the alteration in glycan patterns with VPA treatment.

Furthermore, when combined with the results of lectin microarrays and the transcripts of glycan-related genes simultaneously, we found that alteration in transcript

levels of anabolic enzymes in the N-glycan biosynthesis pathway is associated with corresponding changes in glycan structures of glycoproteins in VPA rats. **Figure 5B** showed the specific activity of MAN2A2 and ST6GAL2 enzymes in the N-glycan biosynthesis. *Man1a2* and *Man2a2* encode α -mannosidases, which could catalyze the trimming of high-mannose glycan and remove the mannose residue of glycan. In VPA-treated rats, α -mannosidases expression was significantly reduced at the mRNA level (*Man1a2*, FC = -1.27; *Man2a2*, FC = -1.30) (**Figure 4C**; **Table 4**), with consequent increased branched high-mannose glycan structures (recognized by ConA lectin). Our lectin microarrays also showed that a decrease in sialylated Gal/GalNAc (recognized by WGA

TABLE 4 The expression changes of glycan genes encoding anabolic enzymes involved in glycosylation in valproic acid (VPA)-induced autism model.

Reg.	Category	Sub-category	Entrez gene ID	Gene symbol	Fold Change	
Down-regulation	GTs	CSGlcA-T	316533	<i>Chpf</i>	-1.21	
		CSGlcA-T	296733	<i>Chpf2</i>	-1.5	
		Fucosyl-T	84597	<i>Fut9</i>	-5.51	
		GalNAc-T	304571	<i>Galnt9</i>	-1.51	
		GalNAc-T	288611	<i>Galnt17</i>	-1.37	
		GalNAc-T	64828	<i>B4galnt1</i>	-1.24	
		GalNAc-T	117108	<i>B3gat1</i>	-1.19	
		GalNAc-T	309105	<i>B4galnt4</i>	-1.16	
		Gal-T	362275	<i>B4galnt5</i>	-1.22	
		GlcNAc-T	29582	<i>Mgat3</i>	-1.19	
		GlcNAc-T	65271	<i>Mgat5</i>	-1.54	
		GlcNAc-T	56819	<i>Extl3</i>	-1.44	
		GlcNAc-T	361368	<i>Large1</i>	-1.29	
		Glc-T	171129	<i>Uggt1</i>	-1.45	
		Man-T	362465	<i>Tmtc1</i>	-1.40	
		Man-T	308519	<i>Dpy19l3</i>	-1.40	
		Sia-T	301155	<i>St6gal2</i>	-1.62	
		Sia-T	364901	<i>St8sia5</i>	-1.36	
		Sia-T	25547	<i>St8sia3</i>	-1.28	
		Xyl-T	64133	<i>Xylt1</i>	-1.59	
	**	245960	<i>Alg10</i>	-1.58		
	**	290794	<i>Tnks</i>	-1.32		
	**	363160	<i>Stt3b</i>	-1.26		
	GHs	Hyaluronidases	367166	<i>Hyal1</i>	-1.44	
		Hyaluronoglucosaminidase	308797	<i>Cemip</i>	-1.51	
		Hyaluronoglucosaminidase	309400	<i>Tmem2</i>	-1.64	
		Lysozomal Enzymes	367562	<i>Gaa</i>	-1.19	
Lysozomal Enzymes		684536	<i>Gba</i>	-1.19		
Mannosidases		295319	<i>Man1a2</i>	-1.27		
Mannosidases		308757	<i>Man2a2</i>	-1.30		
Nucleotide Synthesis		114711	<i>Gne</i>	-1.76		
Up-regulation		GTs	Ribosyltransferase	24465	<i>Hprt1</i>	1.20
			Ribosyltransferase	117544	<i>Ppat</i>	1.35
	Sia-T		363040	<i>St3gal4</i>	1.28	
	**		290029	<i>Pnp</i>	1.36	
	GHs	Fucosidase	292485	<i>Fuca2</i>	1.25	
		Nucleotide Synthesis	294673	<i>Hexb</i>	1.20	
		**	25211	<i>Lyz2</i>	1.39	

**Means sub-category is uncertain.

and MAL-I lectin) corresponded to the down-regulated expression of the *St6gal2* gene (FC = -1.62) (Table 4). Sialyltransferase ST6GAL2 transfers Sia from CMP-sialic acid to Gal β 1/GalNAc structure on glycoproteins. Taken together, the results of our study revealed a relationship between the mRNA levels of anabolic enzymes and the forms of glycans on glycoproteins during prenatal exposure to VPA.

Functional sub-network of differentially expressed genes encoding glycoconjugates

Our transcriptomics results also showed 56 genes encoding glycoconjugates with statistical differences ($p < 0.05$) in VPA-treated rats. GO and KEGG enrichment analysis revealed that these 56 genes were annotated as extracellular matrix

TABLE 5 The expression changes of glycan genes encoding glycoconjugates in valproic acid (VPA)-induced autism model.

Reg.	Category	Entrez gene ID	Gene symbol	Fold change	GO functions	
Down-regulation	Lectins	50687	<i>L1cam</i>	-1.37	Axon guidance receptor activity	
		64202	<i>Calr</i>	-1.20	Calcium ion binding	
	GPI-anchored proteins	288280	<i>Ncam2</i>	-1.58	Axonal fasciculation	
		24586	<i>Ncam1</i>	-1.26	Axonal fasciculation Brain development	
		25356	<i>Cntn2</i>	-1.39	Axonogenesis	
		58920	<i>Gpc1</i>	-1.24	Schwann cell differentiation	
	Proteoglycans	25592	<i>Agrn</i>	-1.51	Chemical synaptic transmission	
		56782	<i>Srgn</i>	-1.29	Apoptotic process	
		54226	<i>App</i>	-1.18	Astrocyte activation	
		GAG binding proteins	29715	<i>Slc8a1</i>	-1.82	Calcium ion export
	65047		<i>Slit1</i>	-1.71	Axon extension involved in axon guidance; Axon guidance	
	83467		<i>Slit3</i>	-1.62	Axon guidance; brain development	
	687064		<i>Col25a1</i>	-1.58	Axonogenesis in innervation; Extracellular matrix organization	
			116683	<i>Efna5</i>	-1.51	Axon guidance; Brain development
			140447	<i>Slc8a2</i>	-1.29	Cellular calcium ion homeostasis Cognition and learning
			310207	<i>Sema5a</i>	-1.19	Axonal fasciculation; Axon extension
		Up-regulation	Lectins	29403	<i>Asgr2</i>	1.91
GAG binding proteins			29366	<i>Serpine2</i>	1.27	Glycosaminoglycan binding
	25352		<i>Sod3</i>	1.26	Copper ion binding	
	25728		<i>Apoe</i>	1.29	Aging	

organization, axon development, and synapse organization (Figure 6A). We further constructed the protein-protein interaction network of differentially expressed glycoconjugates in an attempt to come out with molecular mechanisms in VPA rats. The relationships between the differentially expressed glycoconjugates were revealed from the STRING database, and MCL clustering was performed on the network using a confidence cutoff of 0.4. We noticed that MCL clustering formed two clusters (Figure 6B), and utilized the Cytoscape plugin BiNGO to perform biological process enrichment analysis with the differentially expressed genes of each set (Figures 6C,D). Notably, differentially expressed glycoconjugates in the black set were associated with extracellular matrix organization (GO: 0030198) and extracellular matrix (GO: 0031012). The most significantly enriched gene in the KEGG pathway out of these genes was ECM-receptor interaction (rno04512). In addition, glycoconjugates in the pink set were mainly involved in axon guidance (GO: 0007411), axonal fasciculation (GO: 0007413), and negative chemotaxis (GO: 0050919). Concerning molecular functions, target glycoconjugates were enriched in protein binding (GO: 0005515) especially, heparin-binding (GO: 0008201). The most significantly enhanced KEGG pathway was Axon guidance (rno04360). Overall, the functional

effect of glycoconjugates was mainly correlated to extracellular matrix and axon guidance, which provide insights into the underlying molecular mechanism by which synaptic protein may undergo aberrant glycosylation during prenatal VPA exposure.

Discussion

Here we show for the first time that there are aberrant expressions of glycan patterns and glycan-related genes in an environmentally triggered autism model in rats. Our lectin microarrays showed that high-mannose and Sia α 2-3 Gal/GalNAc structure altered significantly in rats prenatally exposed to VPA. Using RNA-seq technology, 107 glycan-related genes were identified as differentially expressed genes in VPA rats. Some of these genes have been reported as candidate genes related to autism, including *Large1*, *Galnt9*, and *Hs3st5*. A functional study of DEGs encoding anabolic enzymes found that trimming to form the core structure and glycan extension from core structure was primarily affected, which is consistent with alterations in glycan patterns. In addition, functional effect of DEGs encoding glycoconjugates was mainly correlated

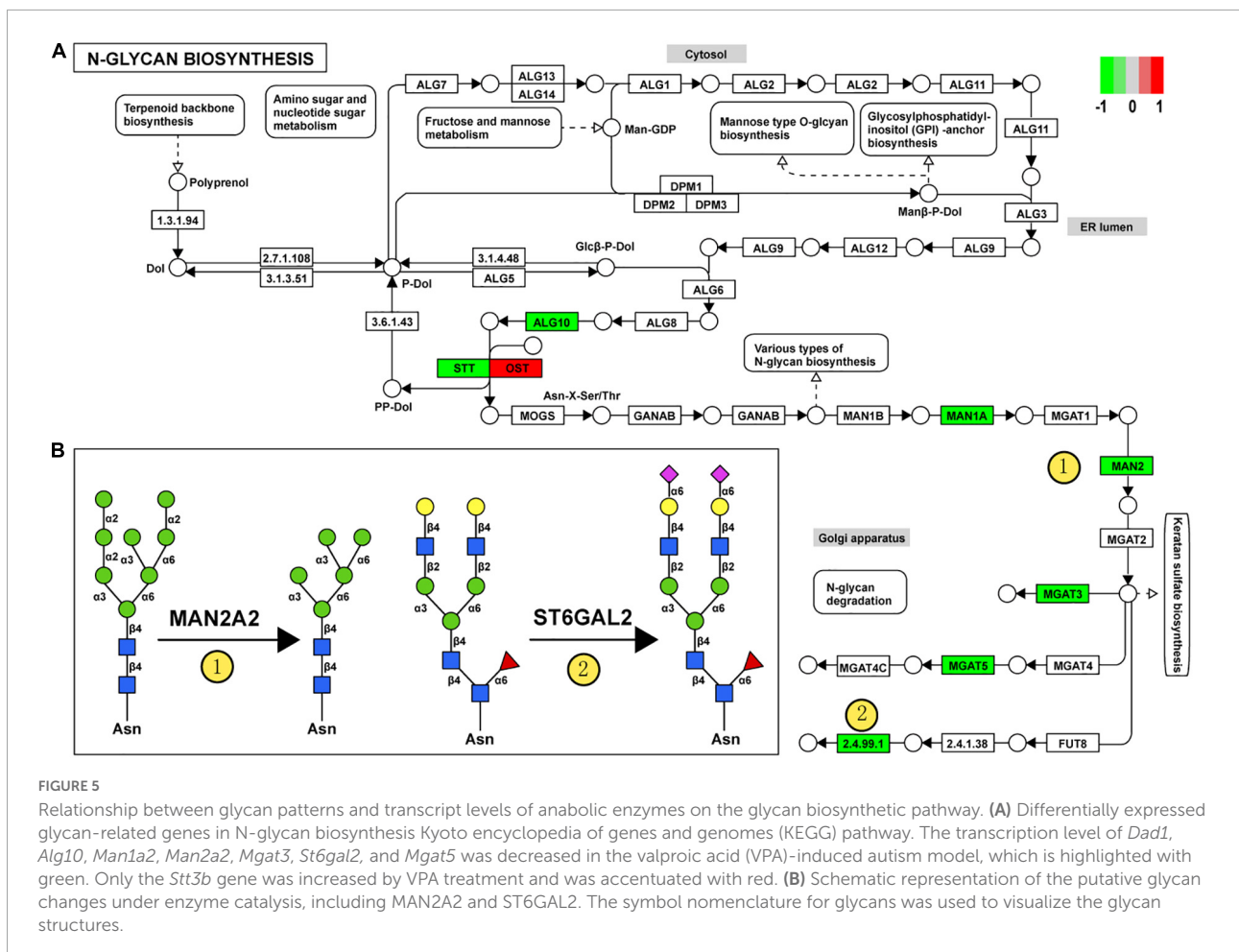


FIGURE 5
 Relationship between glycan patterns and transcript levels of anabolic enzymes on the glycan biosynthetic pathway. **(A)** Differentially expressed glycan-related genes in N-glycan biosynthesis Kyoto encyclopedia of genes and genomes (KEGG) pathway. The transcription level of *Dad1*, *Alg10*, *Man1a2*, *Man2a2*, *Mgat3*, *St6gal2*, and *Mgat5* was decreased in the valproic acid (VPA)-induced autism model, which is highlighted with green. Only the *Stt3b* gene was increased by VPA treatment and was accentuated with red. **(B)** Schematic representation of the putative glycan changes under enzyme catalysis, including MAN2A2 and ST6GAL2. The symbol nomenclature for glycans was used to visualize the glycan structures.

to extracellular matrix and axon guidance. These results provide molecular evidence for the altered expression of genes responsible for the regulation of glycosylation in a VPA-induced rat model of autism.

A significant finding in the present study was that there was 14 lectins expression changes in VPA rats, and some of these alterations in glycan patterns were consistent with the previous publications. Our lectin microarrays showed that ConA was the up-regulation lectin with the most significant fold changes (FC = 1.82; **Table 3**) in VPA-treated rats, which binds to branched high-mannose Man α 1-3Man. Another study also confirmed that prenatal exposure to VPA significantly increased high mannose-type N-glycan patterns in the hippocampal region, which is recognized by tomato lectin and serves as a biomarker for microglial cells (Codagnone et al., 2015). Our results also showed that the expression of terminal GalNAc structure was down-regulated in VPA rats, which is recognized by BPL (FC = -2.06) and VVA (FC = -2.47) (**Figure 3C**; **Table 3**). GalNAc structure is present in the perineuronal net surrounding basket interneurons. Ariza et al. (2018) found the number of basket interneurons slightly decreased in the prefrontal cortex in autism patients, suggesting that GalNAc

structure is down-regulated in the brain tissue of ASD patients. Using lectin microarray analysis, Qin et al. (2017) showed that the expression of Sia α 2-3 Gal/GalNAc (recognized by MAL-I and MAL-II) was significantly changed in serum samples from ASD. Interestingly, the Sia α 2-3 Gal/GalNAc structure (recognized by MAL-I and WGA) in our lectin microarray analysis was significantly down-regulated in the VPA rats. Both of these results suggest that the Sia α 2-3 Gal/GalNAc structure is involved in the molecular mechanism of ASD.

To examine the global regulation of glycan patterns in the environmentally triggered autism model, we systemically investigated the expression profiles of glycan-related genes in a VPA-induced rat model of autism. Three genes that encode anabolic enzymes, which are among the 107 DEGs, have been reported as candidate genes for autism, and they are *Large1*, *Galnt9*, and *Hs3st5* (van der Zwaag et al., 2009). *Large1* gene encodes Large dual-function glycosyltransferase, and the only known protein modified by Large is dystroglycan. Recent works have reported that the length of the Large-glycan can be altered by changes in *Large1* expression, which affects the ligand-binding capacity of α -dystroglycan (van der Zwaag et al., 2009; Dwyer and Esko, 2016). It has also been reported that

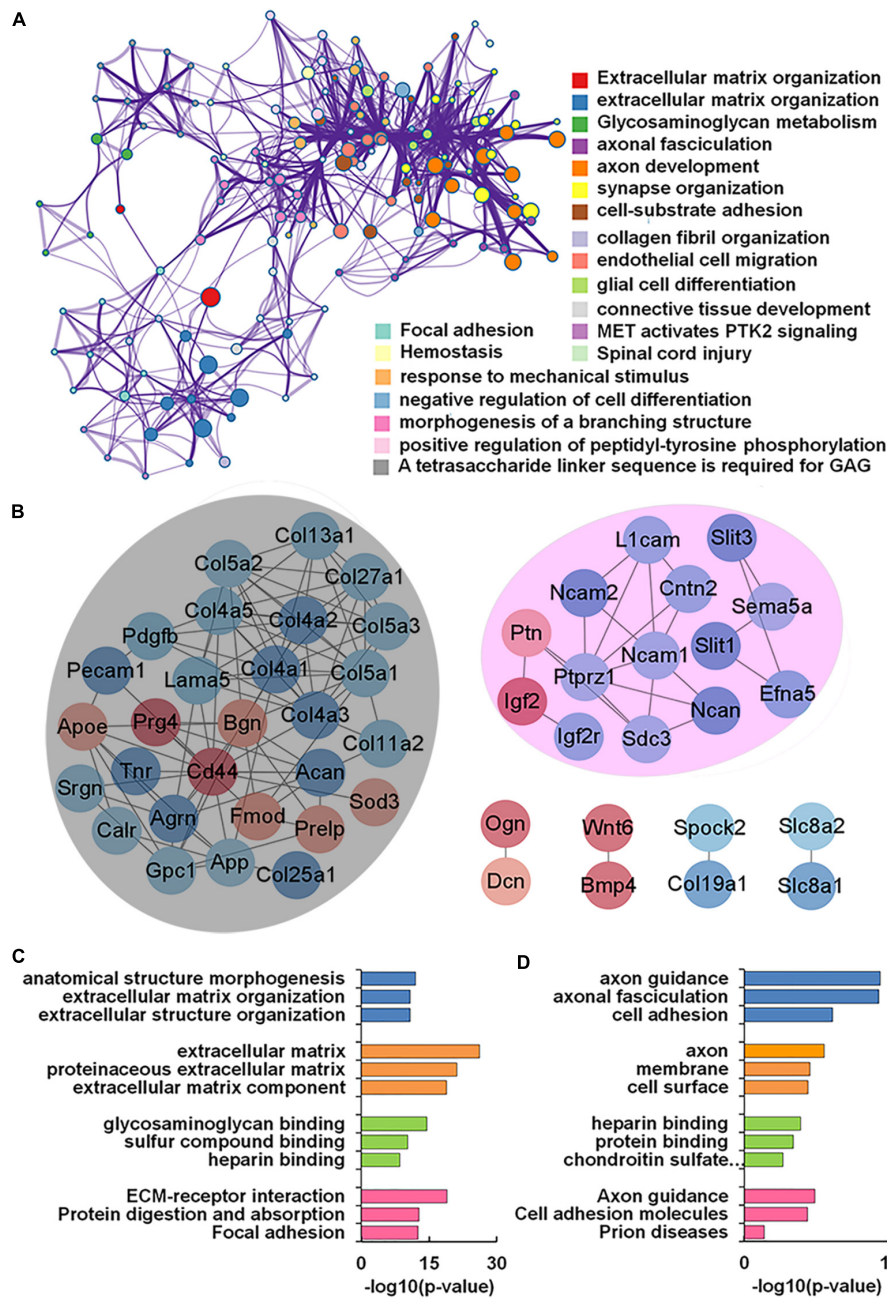


FIGURE 6

Functional network analysis of differentially expressed glycan-related genes (DEGGs) encoding glycoconjugates in valproic acid (VPA)-induced autism model. (A) The enriched network of representative GO terms of 56 DEGGs encoding glycoconjugates using Metascape. (B) Protein-protein interaction network of 56 DEGGs encoding glycoconjugates using Cytoscape software. Red and blue nodes represented up- and down-regulated DEGGs, and the color intensity was proportional to the expression. (C,D) Functional classification of differentially expressed genes of each cluster using Cytoscape plugin BiNGO based on universal GO and KEGG annotation terms.

mutations in the *LARGE1* gene induce abnormal glycosylation of α -dystroglycan and result in congenital muscular dystrophy (Goddeeris et al., 2013). Our expression profiles analysis showed that the *LARGE1* gene was down-regulated in VPA rats (Table 4), indicating that VPA-induced autism is closely related to the abnormal expression of autism candidate genes.

When we combined lectin microarrays and transcriptomics analysis, we found that alterations in gene expression of anabolic enzymes were consistent with changes in glycan patterns in VPA rats. The gene expression changes that encode anabolic enzymes in animal models are also compatible with the lack of function in ASD patients, which may facilitate the exploration

of the association between glycosylation and VPA treatment. As forementioned, our findings demonstrated that ST6GAL2 and its responsible sialylated Gal/GalNAc structures were down-regulated in VPA rats. In addition to ST6GAL2, the down-regulated sialyltransferase genes also included *St8sia5* and *St8sia3* (Table 4). Recently, copy number loss and SNPs in ST8SIA2 have been reported in ASD patients (Demirci et al., 2019). Since ST8SIA5 and ST8SIA3 transfer Sia from CMP-sialic acid to NeuAc α 2/3R or NeuAc α 2/8R structure on glycolipids, it was found that the Sia level of the ASD group was lower than that of the control group (Yang et al., 2018; Demirci et al., 2019). The evidence suggests that the Sia signal pathway may be associated with ASD.

VPA treatment also caused significant changes in the levels of 56 genes encoding glycoconjugates in our glycan-related genes list. Functional enrichment analysis revealed that these 56 DEGs were annotated as extracellular matrix organization, axon development, and synapse organization (Figure 6A). A previous study has confirmed that several genes related to glycoconjugates were markedly disturbed in the animal models of autism. It was reported that the expression of three genes encoding collagens was increased in the mPFC of rats prenatally exposed to VPA (Olde Loohuis et al., 2017). Gasparini et al. (2020) investigated the expression profile of the circular RNAs in the hippocampus of the BTBR T+tf/J mouse model of autism. They found that biological and molecular pathways of hippocampal DEGs were associated with heparan sulfate pathway. Both collagens and heparan sulfate proteoglycan are significant components of the ECM, which is tightly connected to the perineuronal nets (Mansour et al., 2019). Therefore, disturbances in the expression of ECM components could lead to altered signaling, disturbing proper cellular functioning, and, in the case of neurons, abnormal outgrowth and synaptic functioning (Irie et al., 2012; Mutalik and Gupton, 2021). In the VPA animal model, neurons of the mPFC displayed cytoarchitectural alterations (Mansour et al., 2019), excitatory/inhibitory imbalance (Santos-Terra et al., 2022) and altered synaptic plasticity (Rinaldi et al., 2008). Taken together, we found the aberrant expression of glycan patterns and glycan-related genes in the prenatal VPA exposure model of autism. The results provide insights into the underlying cellular mechanism by which synaptic protein may undergo aberrant glycosylation during ASD.

Limitations

However, it should be noted that our study has several limitations. One limitation is that we didn't investigate these alterations of glycan patterns and gene expression in other animal models of ASD (i.e., genetic models). Then, we did not use immunohistochemical staining to identify specific glycan changes. Lectin histochemistry is non-specific because one

lectin can usually recognize multiple types of glycan structures, making it difficult to distinguish the subtle differences in glycan structures. Lack of protein confirmation for the targeted genes and of biochemical determination of the proposed glycan alterations weakens this study. However, the correlation between gene expression of anabolic enzymes and glycan patterns reported by our research are reflected in VPA-induced rat model of autism, which is novel in exploring the molecular mechanism of ASD and need to be further verified in a future research.

Data availability statement

The datasets presented in this study can be found in online repositories. The names of the repository/repositories and accession number(s) can be found in the article/Supplementary material.

Ethics statement

The animal study was reviewed and approved by Animal Care and Use Committee of Shaanxi Normal University.

Author contributions

YL: conceptualization, data curation, and writing—original draft. YD and QZ: methodology and data curation. ZQ: investigation and writing—review and editing. JF: visualization and resources. WR: investigation and supervision. ZW: data curation, conceptualization, and writing—review and editing. YT: conceptualization and writing—review and editing. All authors have read and agreed to the published version of the manuscript.

Funding

This research was supported by the National Natural Science Foundation of China (81971285), Natural Science Foundation of Shaanxi Province (2020JM-305), and the Fundamental Research Funds for the Central Universities (GK202005001, GK202105001, and GK202103155).

Acknowledgments

We thank the Laboratory for Functional Glycomics, College of Life Sciences, Northwest University, Hanjie Yu, for lectin microarray analysis.

Conflict of interest

The authors declare that the research was conducted in the absence of any commercial or financial relationships that could be construed as a potential conflict of interest.

Publisher's note

All claims expressed in this article are solely those of the authors and do not necessarily represent those of their affiliated organizations, or those of the publisher, the editors and the reviewers. Any product that may be evaluated in this article, or

claim that may be made by its manufacturer, is not guaranteed or endorsed by the publisher.

Supplementary material

The Supplementary Material for this article can be found online at: <https://www.frontiersin.org/articles/10.3389/fncel.2022.1057857/full#supplementary-material>

SUPPLEMENTARY TABLE 1

Information and regulation about 107 differentially expressed glycan-related genes (DEGGs) in valproic acid (VPA)-treated rats.

References

- American Psychiatric Association. (2013). *Diagnostic and Statistical Manual of Mental Disorders, Fifth Edition*. Virginia: American Psychiatric Pub. doi: 10.1176/appi.books.9780890425596
- Ariza, J., Rogers, H., Hashemi, E., Noctor, S. C., and Martinez-Cerdeno, V. (2018). The Number of Chandelier and Basket Cells Are Differentially Decreased in Prefrontal Cortex in Autism. *Cereb. Cortex* 28, 411–420. doi: 10.1093/cercor/bhw349
- Blanchard, D. C., Defensor, E. B., Meyza, K. Z., Pobbe, R. L. H., Pearson, B. L., Bolivar, V. J., et al. (2012). BTBR T+tf/J mice: Autism-relevant behaviors and reduced fractone-associated heparan sulfate. *Neurosci. Biobehav. Rev.* 36, 285–296. doi: 10.1016/j.neubiorev.2011.06.008
- Cao, L., Zhou, Y., Li, X., Lin, S., Tan, Z., and Guan, F. (2021). Integrating transcriptomics, proteomics, glycomics and glycoproteomics to characterize paclitaxel resistance in breast cancer cells. *J. Proteomics* 243, 104266. doi: 10.1016/j.jprot.2021.104266
- Codagnone, M. G., Podestá, M. F., Uccelli, N. A., and Reinés, A. (2015). Differential Local Connectivity and Neuroinflammation Profiles in the Medial Prefrontal Cortex and Hippocampus in the Valproic Acid Rat Model of Autism. *Dev. Neurosci.* 37, 215–231. doi: 10.1159/000375489
- Demirci, E., Guler, Y., Ozmen, S., Canpolat, M., and Kumandas, S. (2019). Levels of Salivary Sialic Acid in Children with Autism Spectrum Disorder; Could It Be Related to Stereotypes and Hyperactivity? *Clin. Psychopharmacol. Neurosci.* 17, 415–422. doi: 10.9758/cpn.2019.17.3.415
- Di, Y., Li, Z., Li, J., Cheng, Q., Zheng, Q., Zhai, C., et al. (2021). Maternal folic acid supplementation prevents autistic behaviors in a rat model induced by prenatal exposure to valproic acid. *Food Funct.* 12, 4544–4555. doi: 10.1039/D0FO02926B
- Dwyer, C. A., and Esko, J. D. (2016). Glycan susceptibility factors in autism spectrum disorders. *Mol. Aspects Med.* 51, 104–114. doi: 10.1016/j.mam.2016.07.001
- Freeze, H. H., Eklund, E. A., Ng, B. G., and Patterson, M. C. (2015). Neurological aspects of human glycosylation disorders. *Annu. Rev. Neurosci.* 38, 105–125. doi: 10.1146/annurev-neuro-071714-034019
- Fukuchi, M., Nii, T., Ishimaru, N., Minamino, A., Hara, D., Takasaki, I., et al. (2009). Valproic acid induces up- or down-regulation of gene expression responsible for the neuronal excitation and inhibition in rat cortical neurons through its epigenetic actions. *Neurosci. Res.* 65, 35–43. doi: 10.1016/j.neures.2009.05.002
- Gasparini, S., Del Vecchio, G., Gioiosa, S., Flati, T., Castrignano, T., Legnini, I., et al. (2020). Differential expression of hippocampal circular RNAs in the btbr mouse model for autism spectrum disorder. *Mol. Neurobiol.* 57, 2301–2313. doi: 10.1007/s12035-020-01878-6
- Goddeeris, M. M., Wu, B., Venzke, D., Yoshida-Moriguchi, T., Saito, F., Matsumura, K., et al. (2013). LARGE glycans on dystroglycan function as a tunable matrix scaffold to prevent dystrophy. *Nature* 503, 136–140. doi: 10.1038/nature12605
- Irie, F., Badie-Mahdavi, H., and Yamaguchi, Y. (2012). Autism-like socio-communicative deficits and stereotypies in mice lacking heparan sulfate. *Proc. Natl. Acad. Sci.* 109:5052. doi: 10.1073/pnas.1117881109
- Kanehisa, M., Furumichi, M., Tanabe, M., Sato, Y., and Morishima, K. (2016). KEGG: New perspectives on genomes, pathways, diseases and drugs. *Nucleic Acids Res.* 45, D353–D361. doi: 10.1093/nar/gkw1092
- Kuo, H. Y., and Liu, F. C. (2018). Molecular pathology and pharmacological treatment of autism spectrum disorder-like phenotypes using rodent models. *Front. Cell. Neurosci.* 12:422. doi: 10.3389/fncel.2018.00422
- Lucchina, L., and Depino, A. M. (2014). Altered peripheral and central inflammatory responses in a mouse model of autism. *Autism Res.* 7, 273–289. doi: 10.1002/aur.1338
- Luo, W., Pant, G., Bhavnasi, Y. K., Blanchard, S. G. Jr., and Brouwer, C. (2017). Pathview web: User friendly pathway visualization and data integration. *Nucleic Acids Research* 45, W501–W508. doi: 10.1093/nar/gkx372
- Mabunga, D. F. N., Gonzales, E. L. T., Kim, J., Kim, K. C., and Chan, Y. S. (2015). Exploring the validity of valproic acid animal model of autism. *Exp. Neurobiol.* 24, 285–300. doi: 10.5607/en.2015.24.4.285
- Mansour, Y., Mangold, S., Chosky, D., and Kulesza, R. J. (2019). Auditory midbrain hypoplasia and dysmorphology after prenatal valproic acid exposure. *Neuroscience* 396, 79–93. doi: 10.1016/j.neuroscience.2018.11.016
- Maupin, K. A., Sinha, A., Eugster, E., Miller, J., Ross, J., Paulino, V., et al. (2010). Glycogene expression alterations associated with pancreatic cancer epithelial-mesenchymal transition in complementary model systems. *PLoS One* 5:e13002. doi: 10.1371/journal.pone.0013002
- Muhle, R. A., Reed, H. E., Stratigos, K. A., and Veenstra-VanderWeele, J. (2018). The emerging clinical neuroscience of autism spectrum disorder: A review. *JAMA Psychiatry* 75, 514–523. doi: 10.1001/jamapsychiatry.2017.4685
- Mutalik, S. P., and Gupton, S. L. (2021). Glycosylation in axonal guidance. *Int. J. Mol. Sci.* 22, 5143. doi: 10.3390/ijms22105143
- Nairn, A. V., York, W. S., Harris, K., Hall, E. M., Pierce, J. M., and Moremen, K. W. (2008). Regulation of glycan structures in animal tissues: Transcript profiling of glycan-related genes. *Journal of Biological Chemistry* 283, 17298–17313. doi: 10.1074/jbc.M801964200
- Neelamegham, S., Aoki-Kinoshita, K., Bolton, E., Frank, M., Lisacek, F., Lütteke, T., et al. (2019). Updates to the symbol nomenclature for glycans guidelines. *Glycobiology* 29, 620–624. doi: 10.1093/glycob/cwz045
- Oinam, L., Changarathil, G., Raja, E., Ngo, Y. X., Tateno, H., Sada, A., et al. (2020). Glycome profiling by lectin microarray reveals dynamic glycan alterations during epidermal stem cell aging. *Aging Cell* 19:e13190. doi: 10.1111/acel.13190
- Olde Loohuis, N. F. M., Martens, G. J. M., van Bokhoven, H., Kaplan, B. B., Homborg, J. R., and Aschrafi, A. (2017). Altered expression of circadian rhythm and extracellular matrix genes in the medial prefrontal cortex of a valproic acid rat model of autism. *Prog. Neuropsychopharmacol. Biol. Psychiatry* 77, 128–132. doi: 10.1016/j.pnpbp.2017.04.009

- Pearson, B. L., Corley, M. J., Vasconcellos, A., Blanchard, D. C., and Blanchard, R. J. (2013). Heparan sulfate deficiency in autistic postmortem brain tissue from the subventricular zone of the lateral ventricles. *Behav. Brain Res.* 243, 138–145. doi: 10.1016/j.bbr.2012.12.062
- Qin, Y., Chen, Y., Yang, J., Wu, F., Zhao, L., Yang, F., et al. (2017). Serum glycoprotein and Maackia amurensis lectin-II binding glycoproteins in autism spectrum disorder. *Sci. Rep.* 7:46041. doi: 10.1038/srep46041
- Quesnel-Vallieres, M., Weatheritt, R. J., Cordes, S. P., and Blencowe, B. J. (2019). Autism spectrum disorder: Insights into convergent mechanisms from transcriptomics. *Nat Rev Genet* 20, 51–63. doi: 10.1038/s41576-018-0066-2
- Rinaldi, T., Perrodin, C., and Markram, H. (2008). Hyper-connectivity and hyper-plasticity in the medial prefrontal cortex in the valproic acid animal model of autism. *Front. Neural Circ.* 2:4. doi: 10.3389/neuro.04.004.2008
- Sang, K., Bao, C., Xin, Y., Hu, S., Gao, X., Wang, Y., et al. (2018). Plastic change of prefrontal cortex mediates anxiety-like behaviors associated with chronic pain in neuropathic rats. *Mol. Pain* 14:1744806918783931. doi: 10.1177/1744806918783931
- Santos-Terra, J., Deckmann, I., Carello-Collar, G., Nunes, G. D., Bauer-Negrini, G., Schwingel, G. B., et al. (2022). Resveratrol prevents cytoarchitectural and interneuronal alterations in the valproic acid rat model of autism. *Int. J. Mol. Sci.* 23:4075. doi: 10.3390/ijms23084075
- Schjoldager, K. T., Narimatsu, Y., Joshi, H. J., and Clausen, H. (2020). Global view of human protein glycosylation pathways and functions. *Nat. Rev. Mol. Cell Biol.* 21, 729–749. doi: 10.1038/s41580-020-00294-x
- Tartaglione, A. M., Schiavi, S., Calamandrei, G., and Trezza, V. (2019). Prenatal valproate in rodents as a tool to understand the neural underpinnings of social dysfunctions in autism spectrum disorder. *Neuropharmacol.* 159:107477. doi: 10.1016/j.neuropharm.2018.12.024
- van der Zwaag, B. L., Franke, M., Poot, Hochstenbach, R., Spierenburg, H. A., Vorstman, J. A. S., van Daalen, E., et al. (2009). Gene-network analysis identifies susceptibility genes related to glycobiochemistry in autism. *PLoS One* 4:e5324. doi: 10.1371/journal.pone.0005324
- Varghese, M., Keshav, N., Jacot-Descombes, S., Warda, T., Wicinski, B., Dickstein, D. L., et al. (2017). Autism spectrum disorder: Neuropathology and animal models. *Acta Neuropathologica* 134, 537–566. doi: 10.1007/s00401-017-1736-4
- Völgyi, K., Udvari, E. B., Szabó, ÉR., Györfy, B. A., Hunyadi-Gulyás, É, Medzihradzky, K., et al. (2017). Maternal alterations in the proteome of the medial prefrontal cortex in rat. *J. Proteomics* 153, 65–77. doi: 10.1016/j.jprot.2016.05.013
- Wu, M., Di, Y., Diao, Z., Yao, L., Qian, Z., Wei, C., et al. (2020). Abnormal reinforcement learning in a mice model of autism induced by prenatal exposure to valproic acid. *Behav. Brain Res.* 395:112836. doi: 10.1016/j.bbr.2020.112836
- Yang, X., Li, H., Ge, J., Chao, H., Li, G., Zhou, Z., et al. (2020). The level of GNE and its relationship with behavioral phenotypes in children with autism spectrum disorder. *Medicine* 99, e21013–e21013. doi: 10.1097/MD.00000000000021013
- Yang, X., Liang, S., Wang, L., Han, P., Jiang, X., Wang, J., et al. (2018). Sialic acid and anti-ganglioside antibody levels in children with autism spectrum disorders. *Brain Res.* 1678, 273–277. doi: 10.1016/j.brainres.2017.10.027
- Yu, H., Zhu, M., Qin, Y., Zhong, Y., Yan, H., Wang, Q., et al. (2012). Analysis of glycan-related genes expression and glycan profiles in mice with liver fibrosis. *J. Proteome Res.* 11, 5277–5285. doi: 10.1021/pr300484j
- Zhang, R., Zhou, J., Ren, J., Sun, S., Di, Y., Wang, H., et al. (2018). Transcriptional and splicing dysregulation in the prefrontal cortex in valproic acid rat model of autism. *Reprod. Toxicol.* 77, 53–61. doi: 10.1016/j.reprotox.2018.01.008
- Zhou, J., Zhang, X., Ren, J., Wang, P., Zhang, J., Wei, Z., et al. (2016). Validation of reference genes for quantitative real-time PCR in valproic acid rat models of autism. *Mol. Biol. Rep.* 43, 837–847. doi: 10.1007/s11033-016-4015-x